



Field observations of an evolving rip current on a meso-macrotidal well-developed inner bar and rip morphology

Nicolas Bruneau^{a,b,c,*}, Bruno Castelle^{a,b}, Philippe Bonneton^{a,b}, Rodrigo Pedreros^c, Rafael Almar^{a,b}, Natalie Bonneton^{a,b}, Patrice Bretel^{a,b}, Jean-Paul Parisot^{a,b}, Nadia Sénéchal^{a,b}

^a CNRS, UMR EPOC 5805, Talence, F-33405, France

^b Université de Bordeaux, UMR EPOC 5805, Talence, F-33405, France

^c BRGM, 3 Avenue Claude-Guillemain, BP 36009, 45060 Orléans Cedex2, France

ARTICLE INFO

Article history:

Received 30 June 2008

Received in revised form

21 April 2009

Accepted 13 May 2009

Available online 28 May 2009

Keywords:

Rip current

Meso-macrotidal beach

Field experiment

Mean circulations

Very low-frequency motions

Morphodynamics

ABSTRACT

The Aquitanian Coast (France) is a high-energy meso-macrotidal environment exhibiting a highly variable double sandbar system. The inner and the outer bar generally exhibit a bar and rip morphology and persistent crescentic patterns, respectively. In June 2007, an intense five-day field experiment was carried out at Biscarrosse Beach. A large array of sensors was deployed on a well-developed southward-oriented bar and rip morphology. Daily topographic surveys were carried out together with video imaging to investigate beach morphodynamic evolution. During the experiment, offshore significant wave height ranged from 0.5 to 3 m, with a persistent shore-normal angle. This paper identifies two types of behavior of an observed rip current: (1) for low-energy waves, the rip current is active only between low and mid tide with maximum mean rip current velocity reaching 0.8 m/s for an offshore significant wave height (H_s) lower than 1 m; (2) for high-energy waves ($H_s \approx 2.5$ –3 m), the rip current was active over the whole tide cycle with the presence of persistent intense offshore-directed flows between mid and high tide. For both low and high-energy waves, very low-frequency pulsations (15–30 min) of the mean currents are observed on both feeder and rip channels.

A persistent slow shoreward migration of the sandbar was observed during the experiment while no significant alongshore migration of the system was measured. Onshore migration during the high-energy waves can be explained by different sediment transport processes such as flow velocity skewness, wave asymmetry or bed ventilation. High-frequency local measurements of the bed evolution show the presence of significant (in the order of 10 cm) fluctuations (in the order of 1 h). These fluctuations, observed for both low- and high-energy waves, are thought to be ripples and megaripples, respectively and may play an important but still poorly understood role in the larger scale morphodynamics. The present dataset improves the knowledge of rip dynamics as well as the morphological response of strongly alongshore non-uniform meso-macrotidal beaches.

© 2009 Elsevier Ltd. All rights reserved.

1. Introduction

Rip currents are narrow, intense, seaward-flowing currents which extend beyond the surf zone, and are commonly observed on many beaches. They can transport large quantities of sediment seaward, shape and interact with the sandy shoreline (Thornton et al., 2007). Understanding the dynamics of rip currents remains a scientific challenge for beach hydro and morphodynamics and for human safety. While rips have received increasing attention (MacMahan et al., 2006) in the scientific literature, there are remaining areas of uncertainty due to a lack of field measure-

ments that need to be addressed to improve model validations in topographically-controlled rip current settings.

Various laboratory and field measurements have been carried out during the last decades to understand rip current dynamics. Haas and Svendsen (2002) studied the vertical distribution of rip currents. They found that vertical profiles of horizontal velocities are nearly depth-uniform inside the channel and depth-varying further offshore with higher velocities at the surface than near the bottom. Within field experiments, Brander and Short (2001) mentioned the non-uniform structure of rip currents with maximum velocities occurring in the middle of the water column. A quasi-three-dimensional modeling study was carried out and compared to experimental data by Haas et al. (2003). The authors highlighted the important role of wave/current interactions in rip current systems, particularly for the generation of low-frequency

* Corresponding author.

E-mail address: n.bruneau@epoc.u-bordeaux1.fr (N. Bruneau).

pulsations. Rip current pulsations can arise from wave group forcing at the infragravity band (MacMahan et al., 2004a) and can also be observed in the far-infragravity band (MacMahan et al., 2004b; Bonneton et al., 2006), the latter being referred as very low-frequency (VLF) motions. The spatial distribution of the VLF velocities within rip current systems is still poorly understood. In addition, debates remain about the mechanisms of rip current VLF source (Haller and Dalrymple, 2001; Reniers et al., 2007).

Several authors reported the strong tidal modulation of rip currents, with maximum velocities occurring during low tides (LTs) in micro-mesotidal settings (Brander, 1999; Brander and Short, 2000; MacMahan et al., 2005). Studies on the Aquitanian Coast (Castelle and Bonneton, 2006; Castelle et al., 2006) also showed the presence of strong tidally modulated rip currents with maximum rip velocities close to mid tide (MT) for low-energy waves. High-energy rip currents are still poorly understood, particularly over strongly alongshore non-uniform beaches. Brander and Short (2000) measured mean currents reaching 1 m/s near a rip neck of an oblique sandbar system for moderate/energetic conditions. Documented rip studies have mainly focused on low-energy wave conditions over small alongshore bed non-uniformities, suggesting that low waves could only induce low-energy rip currents with most of these rip current velocities on the order of $\sim 0.2\text{--}0.4\text{ m/s}$ (MacMahan et al., 2006). This present paper aims to study an intense rip current system, for both low- and high-energy waves, over a well-developed inner bar and rip morphology in a meso-macrotidal setting.

Conceptual models have been developed to predict three-dimensional beach changes associated with variations in environmental conditions. The classification schemes presented by Wright and Short (1984) are widely accepted. This conceptual model has been modified by several authors to fit the classification to their own studied beach (Masselink and Short, 1993; Brander, 1999; Castelle et al., 2007). For the Aquitanian Coast, a complete description of the observed and expected morphologies is given in Castelle et al. (2007). In this type of classification, the beaches are divided into three main different states as dissipative, intermediate and reflective (with sub-states). During high-energy conditions, the beach evolves from a more reflective state towards a more dissipative state (up-state transition). These models predict down-state transitions (towards a more reflective state) for low-energy wave conditions. Surprisingly, during the present field experiment, an onshore bar migration was observed during high-energy conditions, which is discussed in this paper.

The double-barred intermediate high-energy Aquitanian Coast beaches exhibit strongly alongshore non-uniform and variable inner bar morphologies (Castelle et al., 2007). Previous rip current studies on the Aquitanian Coast suffered from the lack of measurements in the rip. Despite the overall morphodynamics of the inner bar system being quite well understood (Castelle et al., 2007), areas with a paucity of high sample rate data remain, particularly during high-energy conditions. The present study presents an intensive five-day field experiment undertaken over a well-developed bar and rip morphology exposed to a large range of shore-normal waves ($0.5 < H_s < 3\text{ m}$, where H_s is the significant wave height) and involving a substantial onshore migration of the bar. We show that rip current can be reasonably intense ($\approx 0.8\text{ m/s}$) for low-energy waves ($H_s \approx 0.8\text{ m}$) if the morphology is strongly alongshore non-uniform. Two specific wave events are selected (one during low-energy conditions, one during high-energy conditions) to investigate the evolving rip current system behavior. In addition, the difference of tidal modulation with earlier studies in micro-mesotidal environment settings is discussed. Then, the morphodynamics of the inner bar and rip system is investigated on this meso-macrotidal beach.

2. Field experiment description

2.1. Field site

The field experiment was performed in June 2007, at Biscarrosse Beach (France), located about 10 km southward of the Arcachon Lagoon inlet (Fig. 1). The Aquitanian Coast is a wave-dominated environment, except near the Arcachon Lagoon inlet and the estuaries of Adour and Gironde which are tide-dominated environments. At Biscarrosse Beach, a persistent crescentic subtidal outer bar and an intertidal inner bar and rip morphology are observed most of the time. This wave-dominated beach is exposed to high-energy North Atlantic swells coming mainly from the W–NW direction within offshore wave height reaching 10 m during severe storm. The annual mean H_s is about 1.4 m and the mean period around 6.5 s (Butel et al., 2002). Finally, the annual mean spring tidal range is approximately 3.7 m with maximum tidal range reaching 5 m. While previous studies on Aquitanian Coast beaches were undertaken at Truc Vert Beach (Fig. 1) (Michel and Howa, 1999; Castelle et al., 2006; Masselink et al., 2008; Sénéchal et al., 2009), this experiment took place at Biscarrosse because of the recent implementation of a permanent video imagery station (Almar et al., in press).

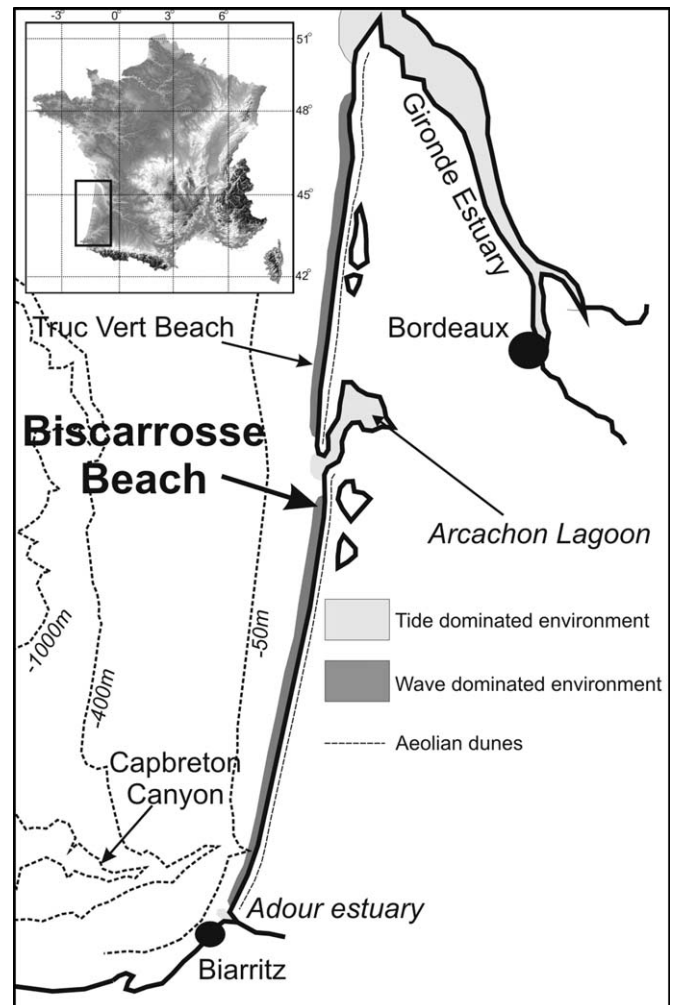


Fig. 1. The French Aquitanian Coast indicating the Biscarrosse field site and locations of wave-dominated and tide-dominated environments.

2.2. Field experiment: Biscarrosse 2007

In high-energy environments like the Aquitanian Coast, the deployment of instruments in the main body of the rip current system is a logistical challenge due to strong currents and the intense morphological evolution. Thus, an array of 12 in-situ stationary instruments (Fig. 2) were deployed on a well-developed inner bar and rip system, in the intertidal zone, between June 13 and June 17. The deployment strategy aimed at capturing the rip current circulation patterns. Four pressure sensors (noted PS1–4, sampled at 8 Hz), four acoustic doppler velocimeter (ADV1–4, 8 Hz), one acoustic Doppler current profiler (ADCP-1, profile interval 20 s), one acoustic wave and currentmeter (AWAC, profile interval 300 s) and one S4 interocean current velocimeter (2 Hz) were deployed. The S4 was deployed in three different locations in the vicinity of the rip neck (Fig. 2, S4-1, -2, -3 correspond to the three deployment locations). Two ADVs (ADV2 and ADV4) and the S4 were deployed in both northern and southern feeder channels and close to the rip channel, respectively. Finally, during the first tide cycle of the experiment, a human drifter experiment was carried out in the rip current system. Table 1 shows the schedule of the sensor deployment as all the instruments were not deployed at the same time.

To measure offshore wave conditions, another ADCP (ADCP-2, 10 min, Fig. 2) was deployed at 10 m depth (at low tide) seaward of the study area. Offshore wave conditions remained very close to shore-normal incidence, favoring rip current formation rather than sinuous longshore currents. Offshore significant wave height ranged from 0.5 to 3 m (Fig. 3) with persistent swell and sometimes a superimposed wind sea. The peak wave period (T_p) ranged from 8 to 11 s. The experiment took place during spring tides, with a tidal range varying from 3.3 to 3.8 m. Thus, in the reference system of coordinates (0 bathymetry), the water level ranged between about 0.9 and 4.7 m.

Daily, topographic surveys were carried out at low tide with 15 m spacing transects on an area covering about 1 km and 250 m in the longshore and cross-shore directions, respectively. The real-time kinematics GPS used herein for measuring the topography with a centimetric precision was a Trimble 5700. In addition, coarser 3 km alongshore topographic surveys were undertaken (25 m spacing transects). To analyze the high-frequency bottom level evolution, an altimeter (ALTUS in Fig. 2, 2 Hz) was placed shoreward of the rip channel. The camera video-imaging system, developed at the NIWA (New Zealand), was implemented in April 2007 at Biscarrosse Beach. The station is composed of five high-resolution cameras which provide high sample rate information of an about 2 km alongshore stretch of beach covering the field experiment area (Almar et al., in press). The “Service Hydrographique et Oceanographique de la Marine Nationale” (SHOM) undertook a large high-resolution bathymetric survey of the area (Fig. 2, bottom right) showing the presence of an almost straight subtidal outer crescentic bar and a well-developed, poorly rhythmic, inner bar and rip morphology.

The instrumented bar and rip morphology was characterized by a narrow and deep rip channel. Fig. 4 describes the studied morphology with the cross-sections of the feeder and rip channels (following the work of Brander and Cowell, 2003). The cross-shore section of the rip-neck channel (Fig. 4b) reached about 110 m wide and 1.4 m deep. Water depth in the rip channel ranged from 1.3 to 5.1 m depending on the tide elevation. The northern longshore-oriented feeder channel was characterized by a cross-section depth and width of around 0.9 and 60 m, respectively (Fig. 4c). The southern longshore-oriented feeder channel was less developed than the northern feeder, with a cross-section depth and width of 0.3 and 50 m, respectively (Fig. 4d). The water depth in both the

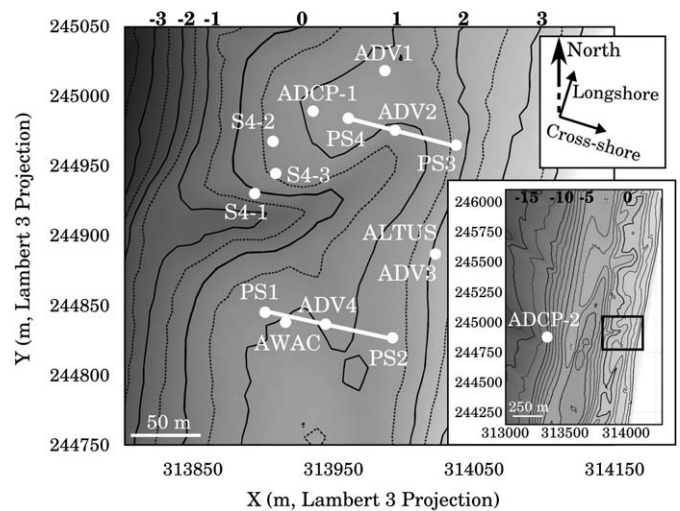


Fig. 2. Bathymetry of the instrumented bar and rip morphology showing the locations of the sensors. The extensive topography-bathymetry of Biscarrosse Beach with the position of the offshore ADCP deployed at 10 m water-depth at low tide is shown in the right hand panel. The system of coordinates is the Lambert 3 projection. The 0 isobath indicates the lowest astronomical tide.

Table 1
Instrumentation deployment schedule during Biscarrosse field experiment.

Sensors	Days of the field experiment									
	13/06/07		14/06/07		15/06/07		16/06/07		17/06/07	
	am	pm	am	pm	am	pm	am	pm	am	pm
ADV1	-	-	-	-	X	X	-	X	X	-
ADV2	-	X	X	X	X	-	X	X	X	-
ALTUS/ADV3	-	-	-	X	X	X	X	-	-	-
ADV4	-	-	X	X	X	X	X	-	-	-
PS-(1,2)	-	-	X	X	X	X	-	-	-	-
PS-3	-	X	X	X	X	-	X	X	X	-
PS-4	-	X	X	X	X	-	-	-	-	-
ADCP-1	-	-	-	X	X	X	X	-	-	-
ADCP-2	X	X	X	X	X	X	X	X	X	X
AWAC	-	-	-	X	X	X	X	X	X	-
S4	-	X1	X2	X2	X3	X3	X3	X3	X3	-

–, no deployment and X, deployment.

northern and southern feeder channels ranged from 0.5 to 4.3 m and from 0.1 to 3.9 m, respectively. The rip current did not extend to the outer bar. This morphology can be identified as a transverse bar and rip morphology (TBR) according to the Wright and Short (1984) classification.

3. Rip current hydrodynamics

3.1. Mean rip current circulation

As detailed previously, two distinct wave events can be clearly identified during the field experiment. The first three days were characterized by low-energy waves. High-energy waves were recorded during the storm event which started during the afternoon of June 15. To investigate the influence of the offshore wave forcing (significant wave height) on the rip current dynamics, two specific hydrodynamic periods were selected (gray bands in Fig. 3): (1) June 15 from 5 to 10.30 h (UT + 2) with low-energy shore-normal waves ($H_s = 0.85$ m, $T_p = 8$ s); (2) June 15

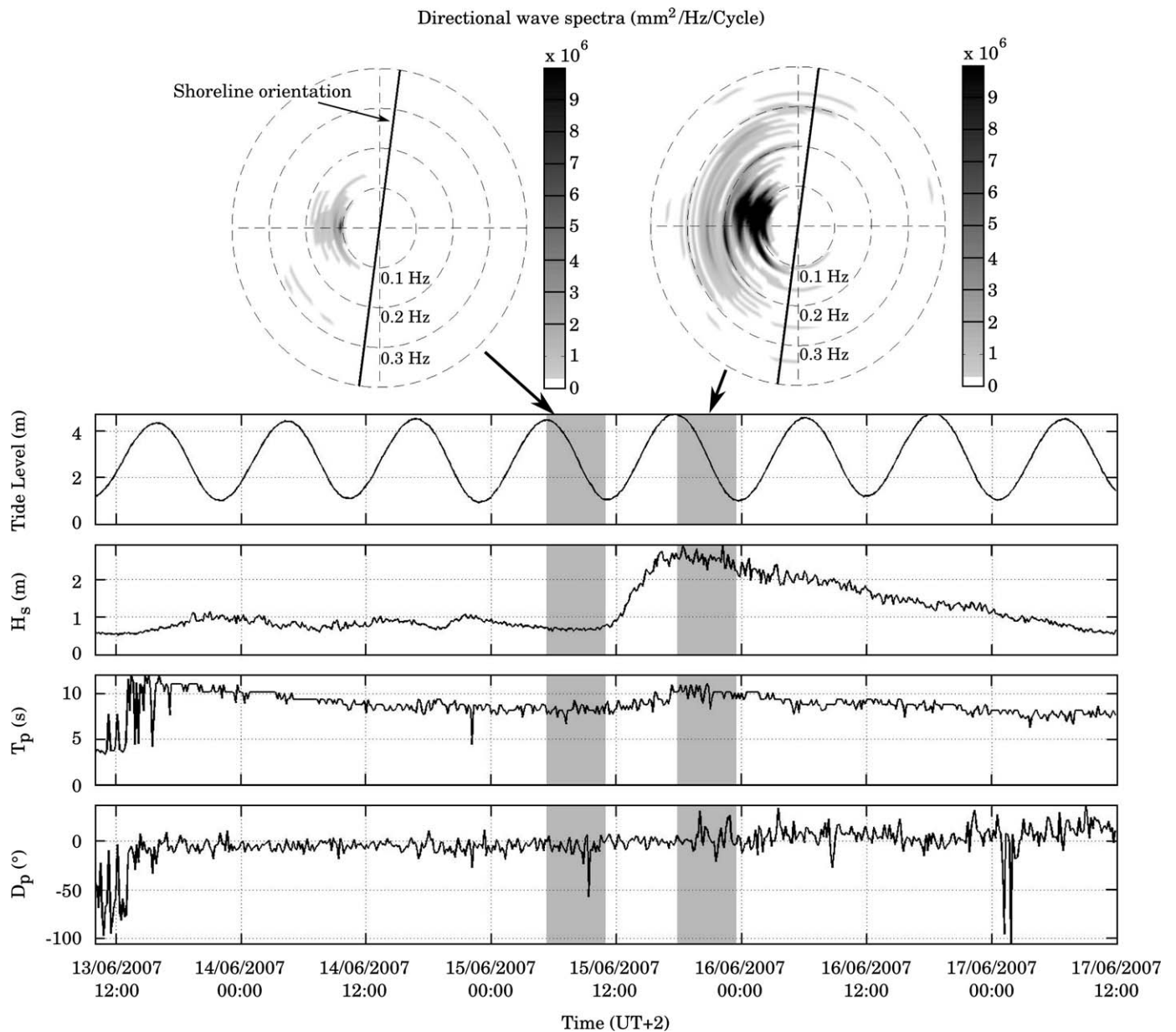


Fig. 3. Offshore wave conditions and tide level measured by the offshore ADCP-2 during the five-day field experiment with indication of the two studied events (shaded areas): (1) June 15 from 5 to 10.30 h (UT + 2) with low-energy shore-normal waves ($H_s = 0.85$ m, $T_p = 8$ s); (2) June 15 from 17 h to 22.30 h (UT + 2) with high-energy shore-normal waves ($H_s = 3$ m, $T_p = 10.5$ s) and superimposed high directional spreading wind sea. The top panels show the directional wave spectrum for each of the two selected events (noted 1 and 2).

from 17 h to 22.30 h (UT + 2) with high-energy shore-normal waves ($H_s = 3$ m, $T_p = 10.5$ s) and superimposed large directional spreading wind sea. Given the strong tidal modulation of observed wave-driven circulations, four representative tidal elevations are selected to investigate the circulation patterns: (1) at high tide (HT), (2) between mid tide and high tide (MHT), (3) at mid tide and (4) between low tide and mid tide (LTMT). For each wave condition, the four tidal elevations have been chosen during falling tide.

The 1-h mean wave-induced currents with superimposed conceptual circulation patterns for the four tidal elevations described before are shown in Figs. 5 and 6 for events 1 and 2, respectively. The mean flows were averaged on a period larger than VLF motions. Both events show a strong tidal modulation of the wave-induced mean circulation patterns. In particular, during event 1, currents were insignificant between mid tide and high

tide as water depth above the bar was too high for the waves break across the bar and to drive rip current circulations. Rip current circulations were significant for lower tide levels (Fig. 5c and d) with persistent onshore flow over the bar on the order of 0.1–0.3 m/s (1-h mean currents), and stronger feeder currents at the southern side of the rip channel. At mid tide, the S4 located on the edge of the main body of the rip channel (S4-3 in Fig. 2) measured 1-h averaged current of about 0.3 m/s and 5-min averaged currents reaching 0.6 m/s (Fig. 7a). Note that for similar wave conditions and with the S4 located closer to the rip channel during the first day of experiment (position S4-1 in Fig. 2, see Fig. 8), mean rip current velocities reached about 0.8 m/s. This suggests that, during event 1, rip current velocities in the main body of the rip channel were larger than those measured by the S4-3. During event 2, mean circulation patterns between low tide and mid tide are similar to those observed during event 1,

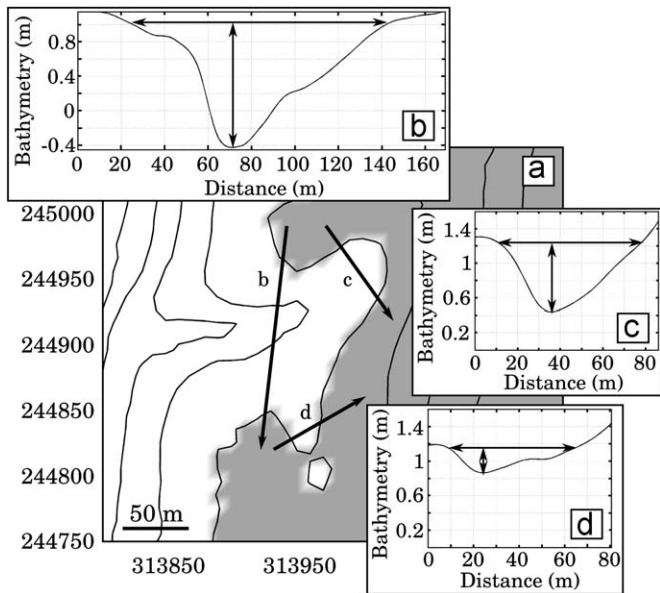


Fig. 4. (a) Description of the bar and rip morphology. Three cross-sections are indicated by the black arrows, (b) cross-section of the rip-neck channel, (c) cross-section of the northern longshore-oriented feeder channel and (d) cross-section of the southern longshore-oriented feeder channel. Black arrows indicate the depth and width of each cross-section.

with more intense velocities (Fig. 6c and d) on the order of 0.3–0.8 m/s for the same tidal water levels. Persistent offshore-directed flows are observed from mid tide to high tide (Fig. 6a and b). The measured mean flow velocities were the result of the superimposition of the rip current circulations and the undertow (also known bed return flow) contribution, as all the current meters were deployed in the surf zone.

Results presented in Fig. 7 show in more detail that, for both high- and low-energy offshore waves, tidal modulation of wave-driven circulation are pronounced. The occurrence of maximum rip current circulation intensity, which is found here to be close to mid/low tide for low-energy waves, shifts toward high tide with increasing wave energy. Strong VLF motions were observed during the whole experiment when the rip current was active.

3.2. Very low-frequency pulsations

Cross-shore and longshore 5-min averaged velocity time series at the S4, ADV3 and ADV4 locations for the two previous events are shown in Fig. 7. The time series corroborate the presence of strong currents for low-energy wave conditions (Event 1, Fig. 7a–c). Velocities measured by the S4 buoy (deployed close to the rip neck but not in the deepest part of the channel) reached 0.6 m/s. Velocities measured in the southern feeder (ADV4) reached 0.4 m/s. During high-energy conditions, 5-min mean currents reached 1.2 and 0.6 m/s, for the rip current and the southern feeder current, respectively (Fig. 7d and e). VLF pulsations were observed when the rip was active. The 15-min pulsations of rip current circulation can be observed for low-energy waves with intensities of about 0.1 m/s (Fig. 7a and b). Fig. 7d and e show 30-min pulsations with intensities on the order of 0.4 m/s (with peak reaching 1 m/s), during the energetic event. Fig. 7c and f illustrate the presence of VLF in the upper beach face where undertow is predominant.

To emphasize the pulsating behavior of rip currents, Fig. 8 shows the velocity spectrum (computed with the S4 measurements recorded during the falling tide June 13 in the after-

noon—gray band in Fig. 8) and the velocity time series measured by the S4 during the first day of the experiment when the S4 was deployed in the very close vicinity of the rip neck (S4-1 in Fig. 2). The 5-min averaged currents (Fig. 8b) clearly show the presence of intense VLF pulsations (six significant peaks are observed during this period for both cross-shore and alongshore velocity components) with intensities reaching 0.6 m/s for significant wave height lower than 1 m (wave conditions similar to event 1). Results show that the energy in the infragravity band was insignificant in comparison with that in the far-infragravity band. Two distinct pulsation periods are identified: around 20 and 30 min. During this first day, a human drifter experiment was carried out with a GPS. All the drifters that were caught in the rip passed over the S4 location (Bruneau et al., 2009) which means that the S4-1 was located in the rip current throat, where rip current velocities were the most intense.

3.3. Vertical structure of the currents

Two vertical current profilers were deployed on the northern and southern bars during the experiment (AWAC and ADCP-1 in Fig. 2). Fig. 9a illustrates the vertical structure of the 30-min mean longshore and cross-shore currents for both low- and high-energy conditions between mid and high tide measured by the AWAC. In both conditions, the profiler measured depth-uniform velocities. Onshore currents were observed for low-energy waves, while strong seaward currents were measured during the storm event. This suggests that flow velocities measured by the other (not profiler) currentmeters were representative of the velocities in the water column. Fig. 9b shows 5-min averaged vertical profile in the afternoon of June 14 when strong onshore wind occurred (~20 m/s), which illustrates the presence of an intense shear near the mean free surface elevation.

4. Morphodynamics

Fig. 10 shows daily geo-referenced rectified images of the bar and rip morphology from June 13 to June 17 in the morning, at low tide. Video imaging and topographic survey analysis show an onshore migration of the oblique bar during the whole field experiment. On June 13 (Fig. 10a), the beach exhibited a well-developed southward-oriented bar and rip morphology. A northward-oriented smaller rip channel was observed in the northern part of the system. Another interesting feature was the presence on the upper part of the beach of a small-scale (about 50 m wide in the cross-shore distance) ridge and runnel system with a shore-normal mini-rip opening facing the main rip channel. Before the storm event (Fig. 10a–c), a quasi-steady onshore migration of the bar of about 5 m/day was observed. During the same time, the mini-rip progressively infilled. Fig. 10d and e show the post-storm evolving beach morphology. Surprisingly, during the storm event, the bar continued to migrate shoreward with a slightly higher rate. The upper part of the intertidal domain was entirely flattened.

High-frequency measurements of the bed evolution were carried out with an altimeter deployed in the upper part of the beach (ALTUS, Fig. 2). Fig. 11 shows the measured bed evolution during both low- and high-energy events. During the low-energy event tide cycle, although the mean currents were weak, the altimeter recorded variations on the order of 1–6 cm with a period of 10–90 min (Fig. 11a). These few centimeter fluctuations may be the trace of migrating ripples. Indeed, given the wave conditions, the ripple predictor of Nielsen (1981) predicts ripples with a 20 cm wavelength, a height of about 3 cm and a migration rate of about 0.04 mm/s, which is realistic for weakly asymmetric waves

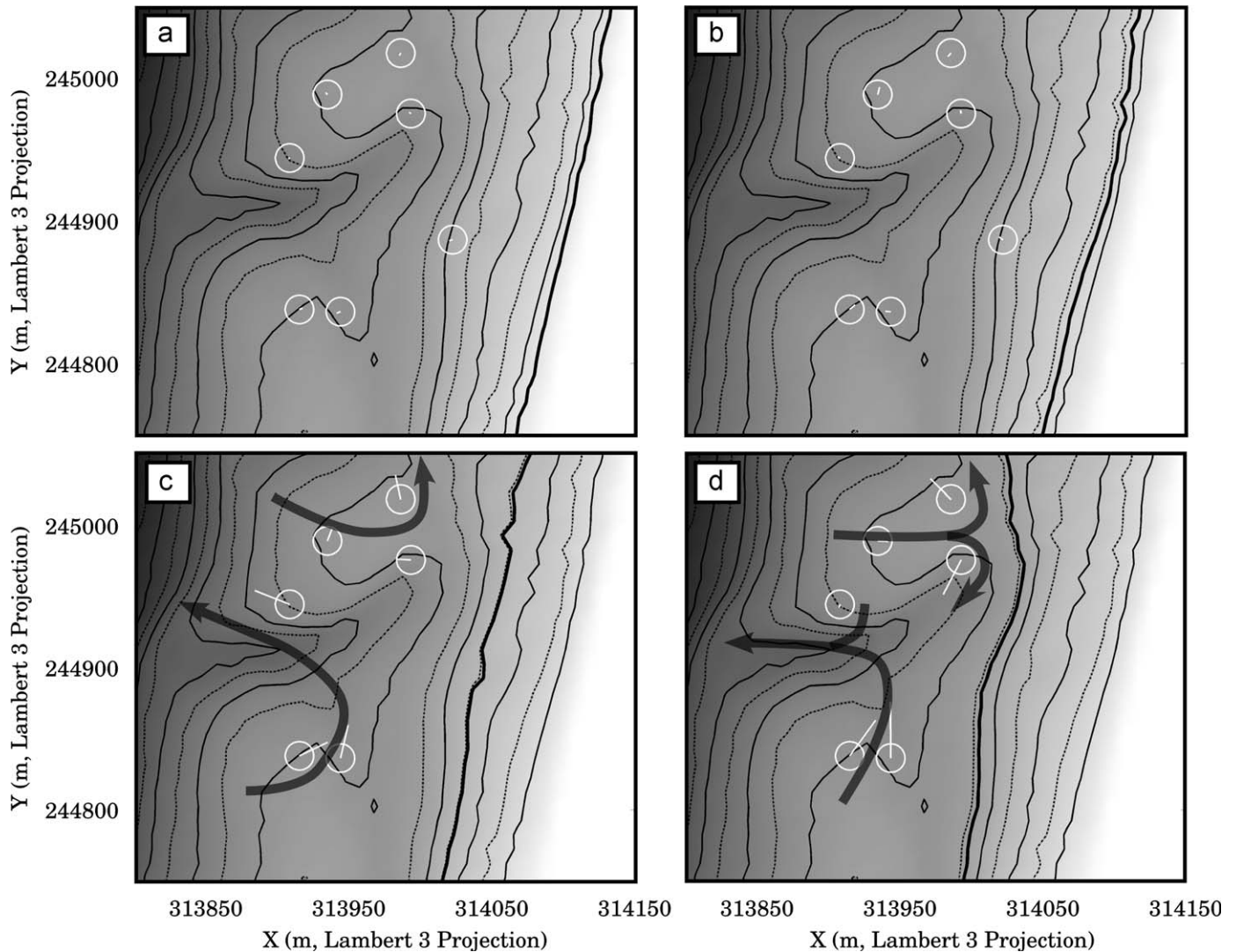


Fig. 5. The 1-h mean current (white line) measured at four different moments of the tide for low-energy wave conditions ($H_s = 0.85$ m, normal incidence and $T_p = 8$ s) during the falling tide of June 15 (from 5 to 11 h (UT + 2), first event in Fig. 3). (a) HT (high tide), (b) MHT (between mid tide and high tide), (c) MT (mid tide) and (d) LTMT (between low and mid tide). Black arrows show the conceptual circulation patterns. The white lines indicate the directions and the intensities of the 1-h mean currents. Current magnitudes of 0.1 m/s are represented by the white circles. The thick black line represents the water level.

at high tide. For the energetic event (Fig. 11b), the bottom level fluctuations reached 20 cm on time scales of about 1 h which cannot be associated to ripples. Indeed, ripple predictors indicate the presence of sheet flow for these current and wave characteristics. In both cases, the net bed level evolution over the tide cycle was only of about a few centimeters (Fig. 11).

5. Discussion

5.1. Hydrodynamics

Drifter experiments in the laboratory (Kennedy and Thomas, 2004) and in the field (MacMahan et al., in press) showed the presence of circulation cells associated with rip currents. The present paper shows, within a large array of measurements, similar results with the presence of two circulations. In general, previous works focusing on rip hydro and morphodynamics were conducted in low-energy environments with relatively small tidal ranges (Sonu, 1972; Smith and Largier, 1995; Aagaard et al., 1997; Brander, 1999; MacMahan et al., 2005, 2006, 2008, in press). Few

studies (Brander and Short, 2000; Castelle et al., 2006) were carried out in more energetic environments (H_s ranging from 1.5 to 2.5 m) where intense rip flow velocities were measured. The present study details a complete dataset on a meso-macrotidal energetic wave-dominated environment. The deployment of the S4 the first day in the close vicinity of the rip neck provided unique information about intensities and VLF motions of rip currents. In particular, intense mean rip current velocities (0.8 m/s) were measured for low-energy conditions ($H_s \approx 0.85$ m) on a well-developed southward-oriented bar and rip system.

Among the studies mentioned above, MacMahan et al. (in press) measured mean rip current velocities of about 0.3 m/s with peak velocities reaching 0.4–0.65 m/s for significant wave height ranging from 0.9 to 1.6 m, over small alongshore bedform non-uniformities. Brander and Short (2000) found mean lagrangian velocities reaching 0.8–1.2 m/s in the rip neck for moderate/energetic conditions. In the present study, rip current velocities during low-energy wave events are stronger than those measured by MacMahan et al. (in press) or similar to those of Brander and Short (2000). Results at Biscarosse Beach are consistent with previous modeling works and field experiments on Aquitanian

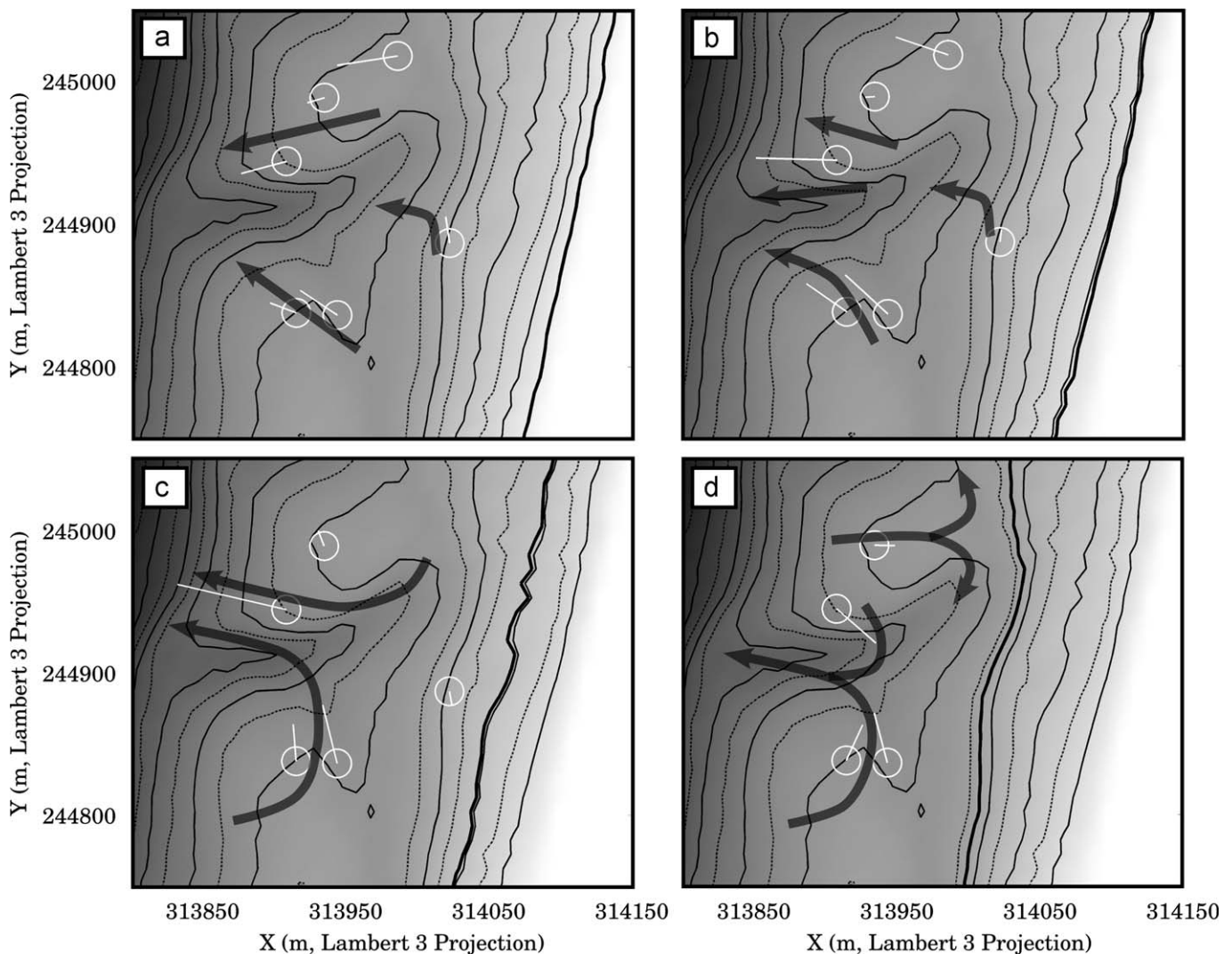


Fig. 6. The 1-h mean current (white line) measured at four different moments of the tide for high-energy conditions ($H_s = 3$ m, normal incidence and $T_p = 10.5$ s) during the falling tide of June 15 (from 17 to 23 h (UT + 2), second event in Fig. 3). (a) HT, (b) MHT, (c) MT and (d) LTMT. Black arrows show the conceptual circulation patterns. The white lines indicate the directions and the intensities of the 1-h mean currents. Current magnitudes of 0.1 m/s are represented by the white circles. The thick black line represents the water level.

Coast (Castelle and Bonneton, 2006; Castelle et al., 2006). The present work highlights the impact of the bathymetry on rip currents and shows that intense rip currents can be observed on strongly alongshore non-uniform beaches even for low-energy waves.

Tidal modulation of rip current identified by few authors (Aagaard et al., 1997; Brander, 1999; MacMahan et al., 2005, 2006; Castelle and Bonneton, 2006; Castelle et al., 2006) is highlighted in the present work. Aagaard et al. (1997), Brander (1999) and MacMahan et al. (2006) showed that flows in the rip channel and feeders are characterized by an increasing speed with decreasing tidal elevation. Aagaard et al. (1997) showed the presence of a wave state threshold suggesting that rip activity is constrained by some critical amount of wave dissipation across the bar. To characterize the occurrence of wave-breaking, Fig. 12 illustrates the ratio of the offshore significant wave height to the local water depth (both in rip channel and above the sandbar). In Fig. 12, the mean currents are insignificant when the ratio is lower than a given threshold (0.35 on the bar). This clearly confirms the presence of a threshold controlling the activity of the rip current system. For low-energy conditions, the threshold is only exceeded between low and mid tide when waves break across the bar while,

during high-energy conditions, the threshold is reached all over the tide cycle. In the present study, when low-energy waves prevailed, maximum rip velocities occurred between low and mid tide which goes with the results of Castelle and Bonneton (2006) and Castelle et al. (2006) using both modeling and experimental studies on other Aquitanian Coast beaches. The occurrence of rip current activity and dynamics is controlled by the rip current system morphology, the offshore wave forcing and the tidal range. The Aquitanian Coast is a meso-macrotidal environment with tidal ranges reaching 5 m during spring tides. At low tide and for a sufficient tidal range, the bar emerges from the water and waves cannot induce feeder and rip currents. When the water level increases, waves break across the bar and drive the rip current circulations. At high tide, low-energy waves do not break across the bar (no rip activity) while energetic waves still break across the bar (rip current activity). This explains why the maximum rip current velocity occurs close to low-mid tide for low-energy waves and shifts to high tide when increasing offshore wave energy. This contrast with earlier rip field studies in lower tidal range settings in which maximum rip current velocity occurred at low tide. The main reason is that the bar did not emerge from the water at low tide.

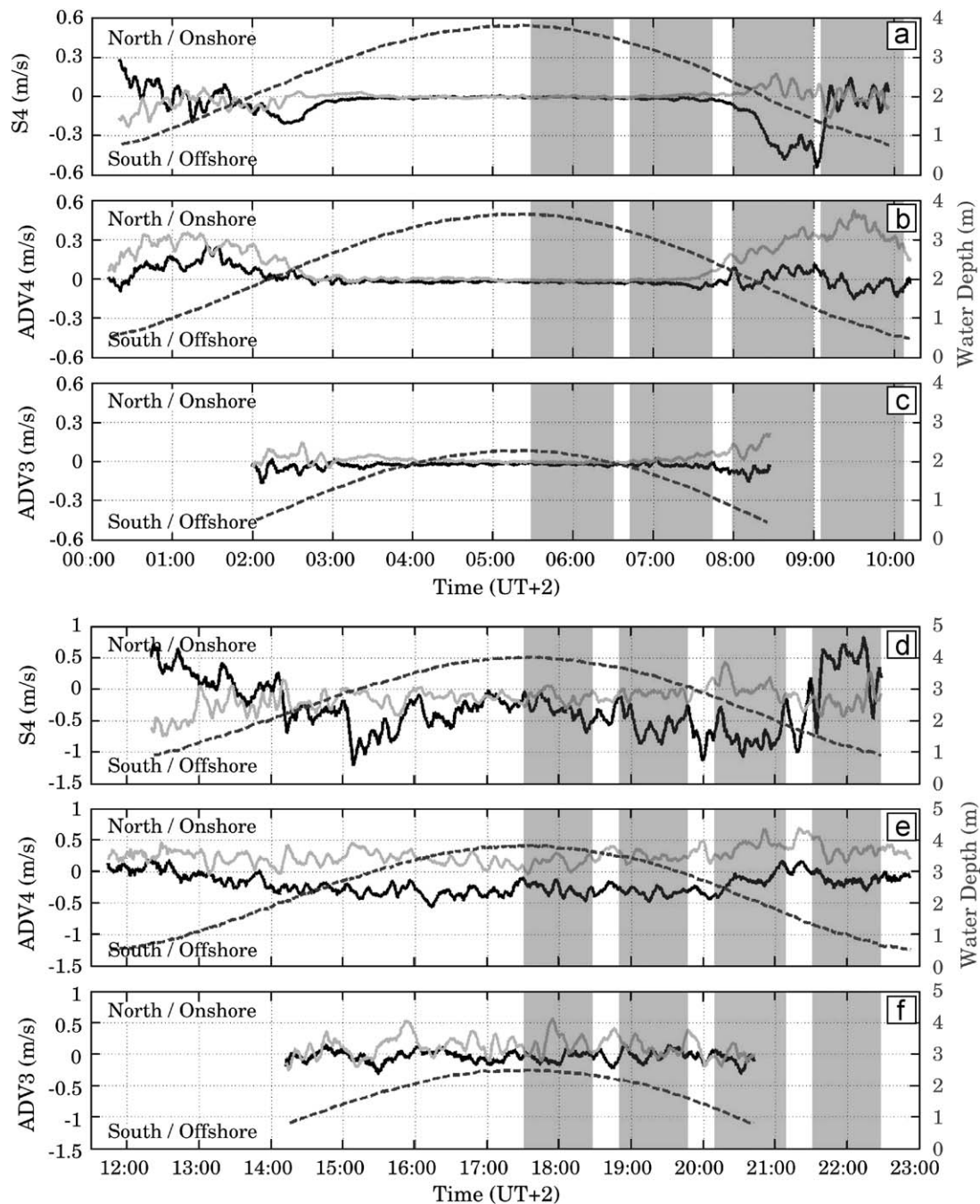


Fig. 7. Flow velocity characteristics on June 15 for the S4 (a, d), the ADV4 (b, e) and ADV3 (c, f). (a, b, c) Time series of 5-min averaged currents for low-energy waves during the first selected event ($H_s = 0.85$ m, normal incidence and $T_p = 8$ s). (d, e, f) Time series of 5-min averaged currents for high-energy waves during the second selected event ($H_s = 3$ m, normal incidence and $T_p = 10.5$ s). The dashed lines represent the water depth. Positive values indicate a shoreward cross-shore current (black) and a northward longshore current (gray).

Recent field experiments (Smith and Largier, 1995; MacMahan et al., 2004a, b, 2006; Bonneton et al., 2006; Reniers et al., 2007) showed infragravity ($0.004 < f < 0.04$ Hz) and/or VLF ($f < 0.004$ Hz) pulsations of rip currents. The present study also underlines the presence of VLF pulsations of the rip currents. The large array of sensors measured both infragravity and VLF motions all over the surf zone, except when the S4 was deployed in the rip throat (S4-1, June 13) when the velocity spectrum clearly highlighted strong energy in the far-infragravity band and insignificant infragravity band contribution. The VLF motions measured in the rip neck reach 0.6 m/s even for low-energy conditions. The results suggest spatial variation of the VLF contribution which is

corroborated by the modeling study of Bruneau et al. (2009). The present study also shows that the period and intensity of the VLF pulsations increase with increasing offshore wave conditions, in agreement with the observations of Callaghan et al. (2004) and MacMahan et al. (2004b) on a transverse barred beach. Finally, the study of the drifter trajectories (Castelle et al., 2008; Bruneau et al., 2009) indicated that 80% of the drifters were retained into the circulation patterns associated with the rip current system and the remaining 20% were caught by a pulsating jet which is in agreement with recent observations of MacMahan et al. (in press) on a micro-mesotidal beach. This corroborates the intense pulsating behavior of rip currents. The generation of the VLF

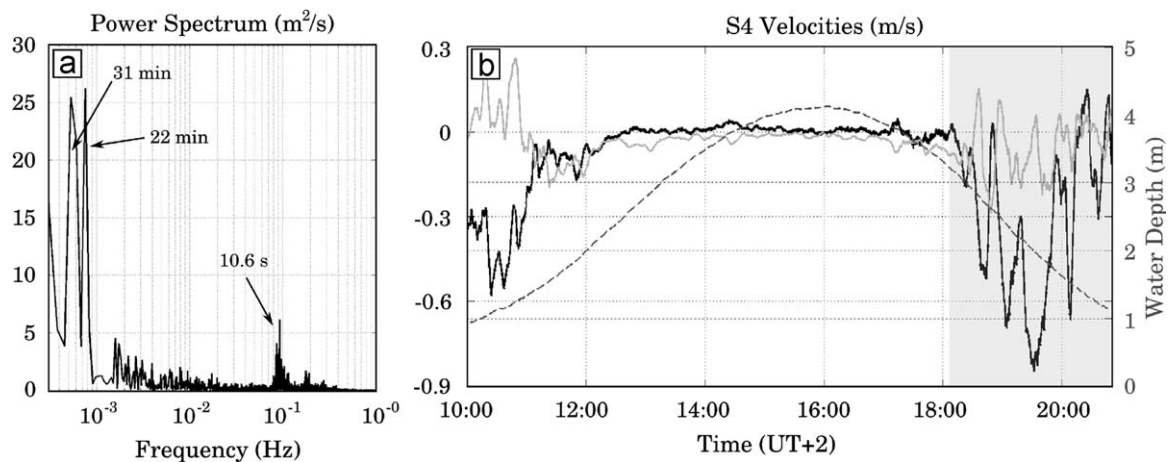


Fig. 8. (a) Velocity power spectrum of rip current measured by the S4 during the afternoon of June 13, when the S4 was deployed in the close vicinity of the rip neck (S4-1 in Fig. 2). (b) The 5-min averaged longshore and cross-shore currents in gray and black, respectively, and superimposed water depth (dashed line). Gray band indicates the section used to compute the spectrum.

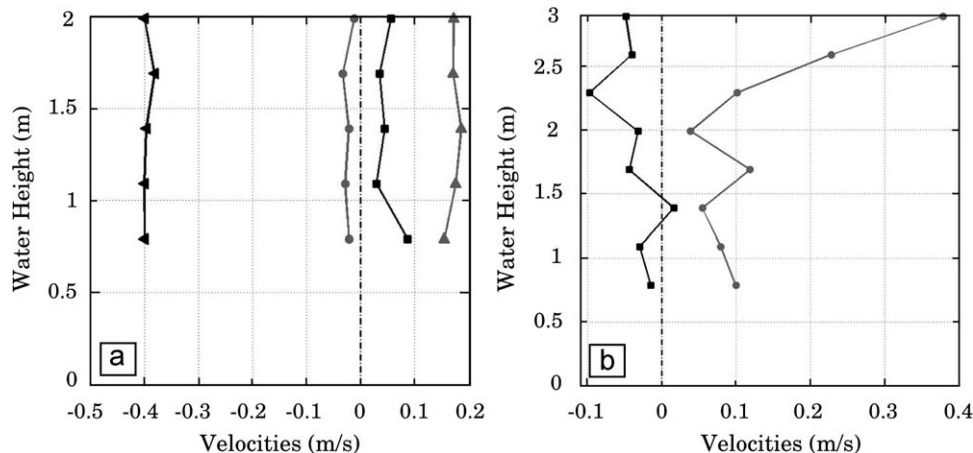


Fig. 9. Vertical profile of averaged current. (a) The 30-min averaged currents measured by the AWAC current profiler between mid tide and low tide. Squares and circles represent the cross-shore and longshore profiles, respectively, during low-energy waves. Triangles represent the profiles during high-energy conditions. (b) The 5-min averaged currents with the presence of wind during calm conditions. Positive values indicate a shoreward cross-shore current (black) and a northward longshore current (gray).

motions are not investigated herein. Understanding the contribution of both wave group (MacMahan et al., 2004b; Reniers et al., 2007) or shear instabilities (Haller and Dalrymple, 2001; Bruneau et al., 2009) is a real scientific challenge to improve our knowledge on the source mechanisms of the VLF.

5.2. Morphodynamics

According to conceptual models (Wright and Short, 1984; Masselink and Short, 1993; Brander, 1999; Castelle et al., 2007), higher wave events result in a rapid up-state transition of beach state, while lower waves result in a slow down-state accretive transition. During the experiment, a shoreward migration of the bar was observed during high-energy waves with H_s reaching 3 m. The observed onshore migration is even more unexpected given that a persistent offshore-directed flow was measured all over the inner bar morphology during the storm. This unexpected onshore bar migration during the storm event can be assumed to be the result of the continuing down-state readjustment of the inner bar resulting from a 6 m storm event which had occurred two weeks before the field campaign. Such accretionary adjustment is in agreement with a previous observation at Truc Vert Beach on the

Aquitainian Coast during PNEC 2001 experiment (Castelle et al., 2006, 2007). Recently, Austin et al. (2009) underlined three processes which can cause a net onshore sediment transport: flow velocity skewness, wave asymmetry and bed ventilation. Wave asymmetry or flow acceleration can induce a net onshore transport even in the presence of seaward mean currents. Finally, other recent studies such as Aagaard et al. (2006) or van Maanen et al. (2008) suggest that the bore dynamics in very shallow water (and in swash zone) is responsible for a significant onshore bar migration which may play an important role in the net cross-shore bar migration over a tide cycle. In the present study, given that flow measurements were acquired at about 50 cm above the seabed, there was no information on hydrodynamics when swash processes were predominant.

During the experiment, the altimeter revealed the presence of significant fluctuations of the bed during a tide cycle. This kind of seabed fluctuations has been observed all over the experiment, both inside and outside the surf zone, and for both low- and high-energy conditions. These results provide quite valuable measurements in an energetic wave-dominated environment. During the low-energy period, seabed fluctuations of few centimeters were measured. For such wave conditions, regarding the main ripple characteristics (wavelength, height and migration speed)

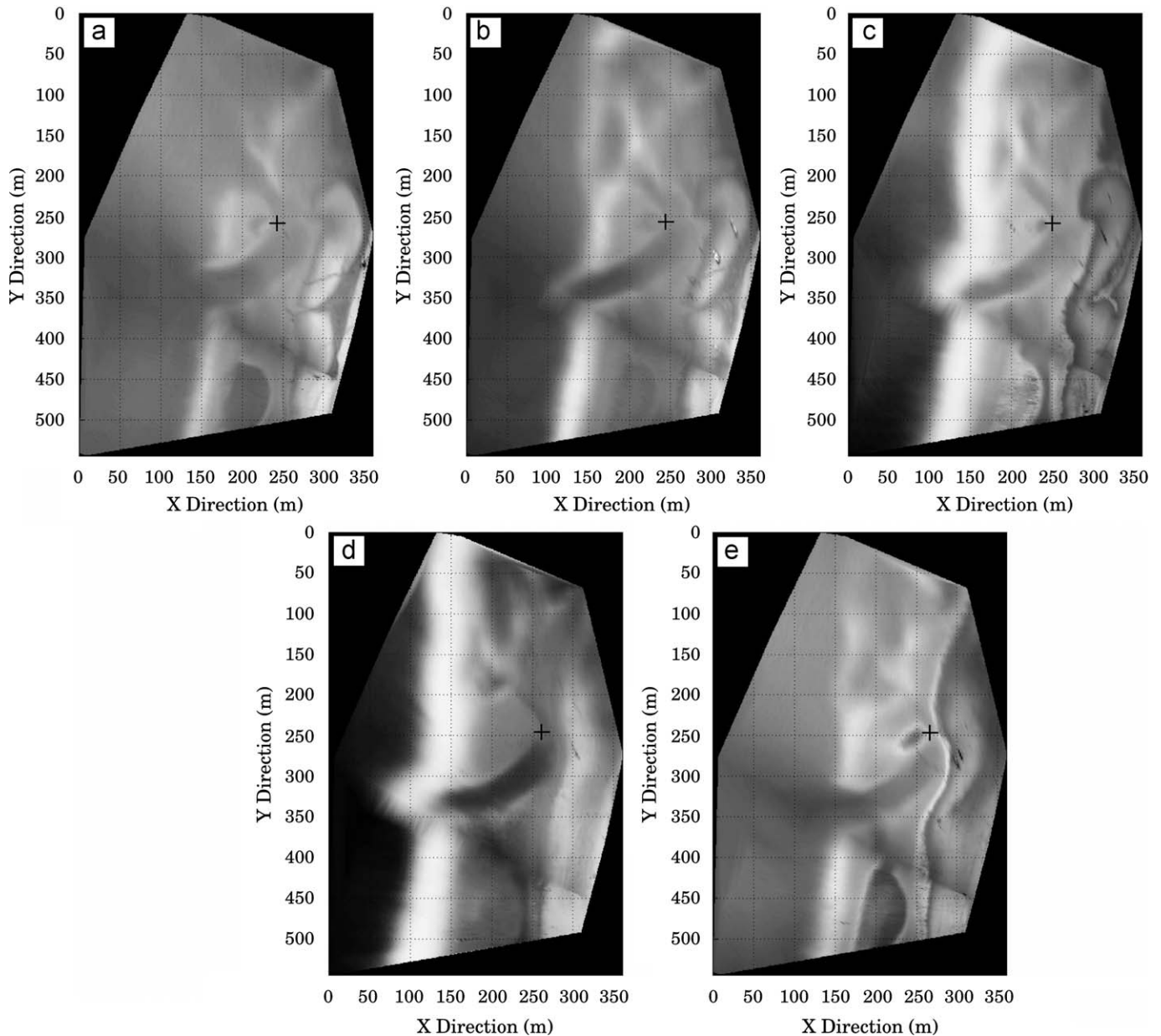


Fig. 10. The 15-min mean camera images (NIWA) combined (cameras 2 and 4) and rectified for each day at low tide during the field experiment centered of the bar and rip system investigated in this study. (a) June 13, (b) June 14, (c) June 15, (d) June 16 and (e) June 17. The black square symbol indicates the position of the bar crest. The time evolution of the crest shows a quasi-steady shoreward migration of about 5 m/day.

given by the Nielsen (1981) ripple predictor, these fluctuations can be caused by migrating ripples. The presence of such bedforms is corroborated by the work of Masselink et al. (2008) in the same environment (Truc Vert Beach). Within two sand ripple profilers, Masselink et al. (2008) observed ripples on the inner bar during calm wave conditions similarly to our observations. In contrast, recorded fluctuations during the energetic event cannot be identified as ripples due to the presence of sheet flow. On a barred beach, Gallagher et al. (1998) measured megaripples in the surf zone with heights of 0.1–0.5 m and widths of 1–5 m for a large range of wave heights (from 0.1 to 4 m) and mean currents (0–2 m/s). Average migration speeds ranged from 0.1 to 1.7 m/h. Wave and flow conditions measured during our experiment and bedform characteristics fit with the observations of Gallagher et al. (1998). This suggests the possibility of megaripple presence. Further measurements of bedform generation and propagation in wave-dominated sandy

beach environment have to be done, particularly in meso-macrotidal environments, to identify their potential role in the larger-scale bar dynamics. For example a refined network of altimeters would provide important information on the spatial variabilities of these fluctuations and would help in identifying their natures and their dynamics.

6. Conclusions

The field experiment detailed in the present work provides a unique in-situ dataset on a meso-macrotidal high-energy rip current system. An intense tidal modulation for low-energy conditions was observed with maximum feeder and rip current velocities occurring between low and mid tide. For high-energy waves, the rip current was active during the whole tide cycle. A

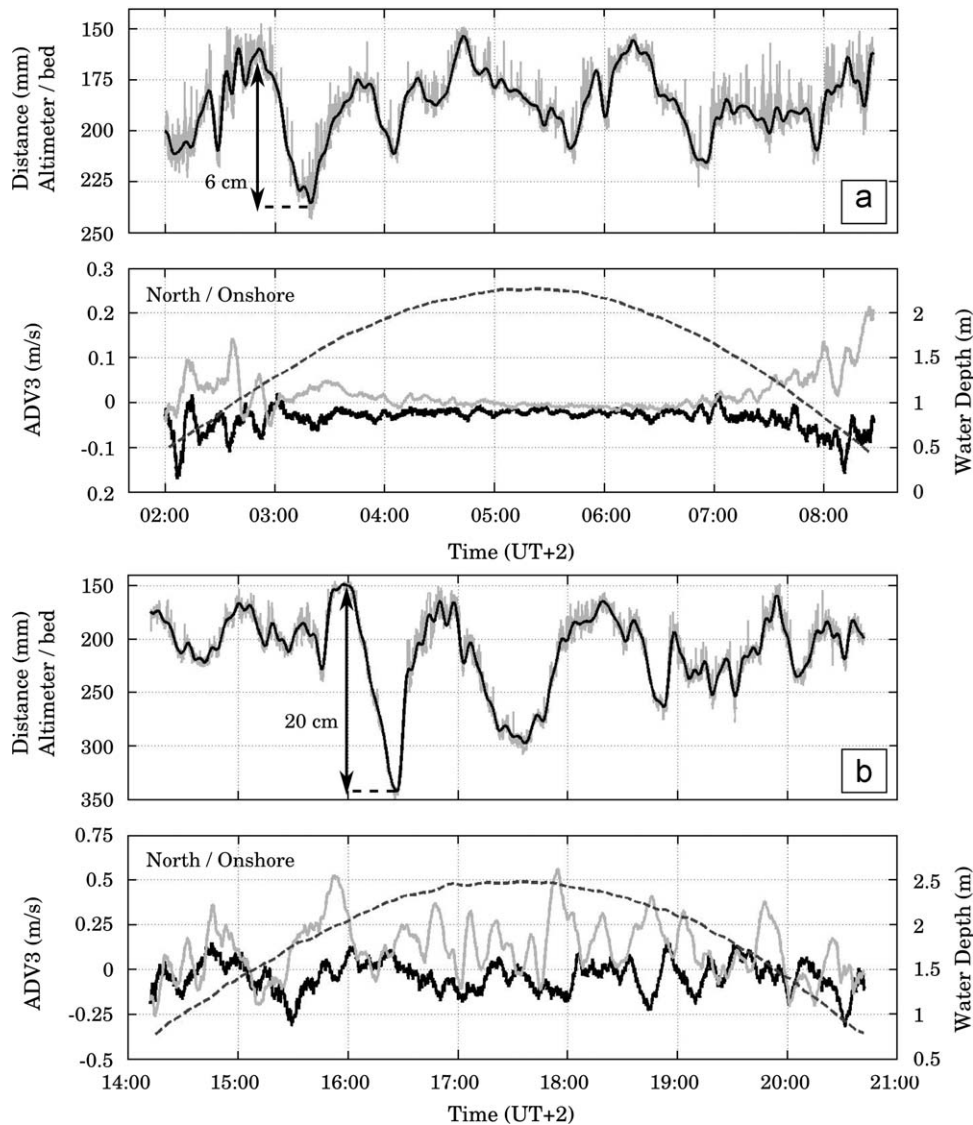


Fig. 11. Time series of the 5-min averaged bed level evolution (black) measured by the altimeter and water depth (dashed line) with superimposed 5-min averaged velocities near the bottom; (a) for low-energy conditions and (b) for energetic conditions.

threshold is identified to characterize rip current activity as a function of offshore wave height and local water depth.

Intense VLF motions of the rip current are also highlighted. The energy of the far-infragravity band can be stronger than this in the infragravity band. In the rip throat when the rip current was active, the infragravity contribution was even found to be insignificant. Intensities and periods of the VLF pulsations reach 0.6 m/s and 15–30 min, respectively, for low-energy conditions ($H_s < 1$ m).

The morphodynamic evolution of this bar and rip morphology was investigated. Using video imagery, we identified a quasi-steady onshore migration of the bar during both low-energy and high-energy conditions. During the high-energy conditions, this onshore bar migration may be explained by sediment transport processes such as velocity skewness, wave asymmetry or in/exfiltration (Austin et al., 2009), that may play a key role in beach morphodynamics; in particular during storm waves when undertow was previously thought to govern the net cross-shore sediment transport.

Finally, the measurements acquired during the Biscarrosse campaign constitute a high quality dataset that will also be useful

for model calibration. Previous to this field measurement, high-frequency measurements of wave-induced currents and morphological evolution at a strongly alongshore non-uniform sandy beach were lacking, particularly in meso-macrotidal settings. In addition, the persistent offshore shore-normal wave incidence allows to characterize the rip currents and associated circulations (Bruneau et al., in press) for a large range of offshore wave energy for numerical models to be confronted with.

Acknowledgments

This Biscarrosse 2007 campaign was carried out thanks to the financial support of the BRGM. This study was performed within the framework of the ECORS (SHOM) project and the MODLIT (SHOM and INSU) project that have also sponsored this work. The authors wish to thank all the teams and students involved in the experiment. In particular, they are grateful to Stéphane Bujan, Déborah Idier, Emmanuel Rommieu, Benjamin Francois, Hervé Michallet, Jean-Marc Barnoud, David Hurther, Francois-Xavier Chassagneux, Fabrice Gouaud, Florent Grasso, Frederic Villiers,

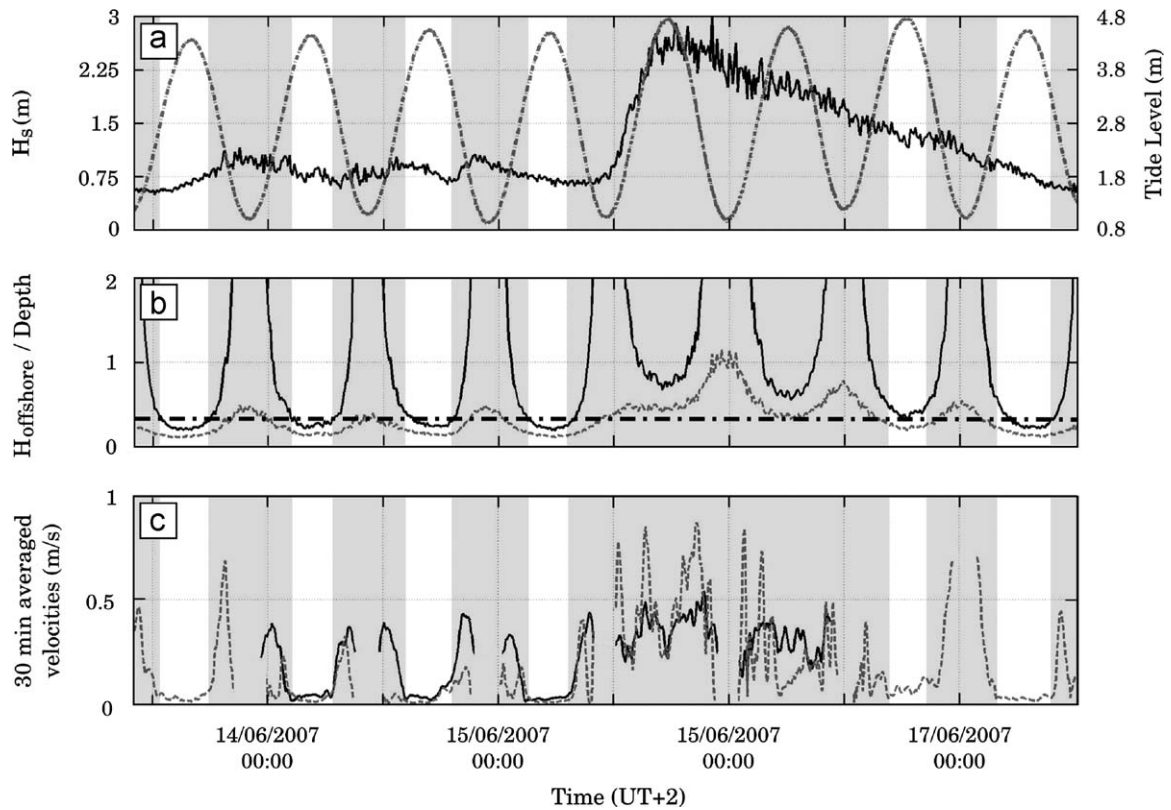


Fig. 12. (a) Offshore significant wave height (black) with superimposed tide level (dashed gray). (b) Ratio of the offshore significant wave height to the local water depth on the bar (black) and in the rip channel (gray). Dashed dot line indicates a threshold (0.35) delimiting rip current activity. (c) The 30-min averaged current magnitudes measured by the ADV4 (black) and by the S4 (gray dashed). Finally the shaded areas illustrate when rip currents are active.

Pierre Ferrer, Simon Morisset, Mathieu Mory, Gael Arnaud, Emanuele Terrile, Silvia Falchetti, Vincent Marieu and Aurélie Dehouck. They also thank the French Navy (SHOM) for the large bathymetry survey carried out on the studied field. Finally, we dedicate this work to our friend and colleague Denis Michel who tragically passed away during this field experiment.

References

- Aagaard, T., Greenwood, B., Nielsen, J., 1997. Mean currents and sediment transport in a rip channel. *Marine Geology* 140, 25–45.
- Aagaard, T., Hughes, M., Møller-Sørensen, R., Andersen, S., 2006. Hydrodynamics and sediment fluxes across an onshore migrating intertidal bar. *Journal of Coastal Research* 22, 247–259.
- Almar, R., Sénéchal, N., Bonneton, P., Roelvink, J. Wave celerity from video imaging: validation with in-situ pre-ecors data. In: 31st International Conference on Coastal Engineering (ICCE 2008), Hamburg, Germany, in press.
- Austin, M., Masselink, G., O'Hare, T., Russell, P., 2009. Onshore sediment transport on a sandy beach under varied wave conditions: flow velocity skewness, wave asymmetry or bed ventilation? *Marine Geology* 59, 86–101.
- Bonneton, N., Bonneton, P., Sénéchal, N., Castelle, B., 2006. Very low frequency rip current pulsations during high energy wave conditions on a meso-macro tidal beach. In: Proceedings of the 30th International Conference on Coastal Engineering, ASCE, United States, pp. 1087–1096.
- Brander, R.W., 1999. Field observations on the morphodynamic evolution of low wave energy rip current system. *Marine Geology* 157, 199–217.
- Brander, R.W., Cowell, P.J., 2003. A trend-surface technique for discrimination of surf-zone morphology: rip current channels. *Earth Surface Processes and Landforms* 28, 905–918.
- Brander, R.W., Short, A.D., 2000. Morphodynamics of a large-scale rip current system at Muriwai Beach, New Zealand. *Marine Geology* 165, 27–39.
- Brander, R.W., Short, A.D., 2001. Flow kinematics of low-energy rip current systems. *Journal of Coastal Research* 17, 468–481.
- Bruneau, N., Castelle, B., Bonneton, P., Pedreros, R., 2009. Very low frequency motions of a rip current system: observations and modeling. *Journal of Coastal Research* SI 56, 1731–1735. Proceedings of the 10th International Coastal Symposium, Lisbon, Portugal.
- Bruneau, N., Castelle, B., Bonneton, P., Pedreros, R., Parisot, J.-P., Sénéchal, N. Modelling of high-energy rip current during Biscarrosse field experiment. In: 31st International Conference on Coastal Engineering (ICCE 2008), Hamburg, Germany, in press.
- Butel, R., Dupuis, H., Bonneton, P., 2002. Spatial variability of wave conditions on the French Aquitanian Coast using in-situ data. *Journal of Coastal Research* 36, 96–108.
- Callaghan, D.P., Baldock, T.E., Nielsen, P., Hanes, D.M., Hass, K., MacMahan, J.H., 2004. Pulsing and circulation in a rip current system. In: Proceedings of the 29th International Conference on Coastal Engineering, ASCE, Portugal, pp. 1493–1505.
- Castelle, B., Almar, R., Bonneton, N., Bonneton, P., Bretel, P., Bujan, S., Bruneau, N., Parisot, J.-P., Pedreros, R., Sénéchal, N., 2008. Dynamics of a moderate-energy rip current over transverse bar and rip morphology: Biscarrosse 2007 field experiment. In: XI International Symposium on Oceanography of the Bay of Biscay, San Sebastián, Spain, pp. 157–158.
- Castelle, B., Bonneton, P., 2006. Modelling of a rip current induced by waves over a ridge and runnel system on the Aquitanian Coast, France. *C.R. Geoscience* 338, 711–717.
- Castelle, B., Bonneton, P., Dupuis, H., Sénéchal, N., 2007. Double bar beach dynamics on the high-energy meso-macrotidal French Aquitanian Coast: a review. *Marine Geology* 245, 141–159.
- Castelle, B., Bonneton, P., Sénéchal, N., Dupuis, H., Butel, R., Michel, D., 2006. Dynamics of wave-induced currents over an alongshore non-uniform multiple-barred sandy beach on the Aquitanian coast, France. *Continental Shelf Research* 26, 113–131.
- Gallagher, E.L., Elgar, S., Thornton, E.B., 1998. Megaripple migration in a natural surf zone. *Letters to Nature* 394, 165–168.
- Haas, K.A., Svendsen, I.A., 2002. Laboratory measurements of the vertical structure of rip currents. *Journal of Geophysical Research* 107 (C5) 2047, doi:10.1029/2001JC000911.
- Haas, K.A., Svendsen, I.A., Haller, M., Zhao, G., 2003. Quasi-three-dimensional modeling of rip current system. *Journal of Geophysical Research* 108 (C7), 3217, doi:10.1029/2002JC001355.
- Haller, M.C., Dalrymple, R.A., 2001. Rip current instabilities. *Journal of Fluid Mechanics* 433, 161–192.
- Kennedy, A.B., Thomas, D., 2004. Drifter measurements in a laboratory rip current. *Journal of Geophysical Research* 109 (C08005), doi:10.1029/2003JC001927.
- MacMahan, J.H., Reniers, A.J.H.M., Thornton, E.B., Stanton, T.P., 2004a. Infragravity rip current pulsations. *Journal of Geophysical Research* 109 (C01033), 1–9.
- MacMahan, J.H., Reniers, A.J.H.M., Thornton, E.B., Stanton, T.P., 2004b. Surf zone eddies coupled with rip current morphology. *Journal of Geophysical Research* 109 (C07004), doi:10.1029/2003JC002083.
- MacMahan, J.H., Thornton, E.B., Reniers, A.J.H.M., 2006. Rip current review. *Coastal Engineering* 53, 191–208.

- MacMahan, J.H., Thornton, E.B., Reniers, A.J.H.M., Stanton, T.P., Symonds, G., 2008. Low-energy rip currents associated with small bathymetric variations. *Marine Geology* 255, 156–164.
- MacMahan, J.H., Thornton, E.B., Stanton, T.P., Measurement of rip current circulation, diffusion and dispersion. In: 31st International Conference on Coastal Engineering (ICCE 2008), Hamburg, Germany, in press.
- MacMahan, J.H., Thornton, E.B., Stanton, T.P., Reniers, A.J.H.M., 2005. RIPEX—rip currents on a shore-connected shoal beach. *Marine Geology* 218, 113–134.
- Masselink, G., Austin, M., Tinker, J., O'Hare, T., Russell, P., 2008. Cross-shore sediment transport and morphological response on a macro-tidal beach with intertidal bar morphology, Truc Vert, France. *Marine Geology* 251, 141–155.
- Masselink, G., Short, A.D., 1993. The effect of tide range on beach morphodynamics and morphology: a conceptual beach model. *Journal of Coastal Research* 9, 785–800.
- Michel, D., Howa, H., 1999. Short-term morphodynamic response of a ridge and runnel system on a mesotidal sandy beach. *Journal of Coastal Research* 15, 428–437.
- Nielsen, P., 1981. Dynamics and geometry of wave-generated ripples. *Journal of Geophysical Research* 86, 6467–6472.
- Reniers, A.J.H.M., MacMahan, J.H., Thornton, E.B., Stanton, T.P., 2007. Modeling of very low frequency motions during RIPEX. *Journal of Geophysical Research* 112 (C07013).
- Sénéchal, N., Gouriou, T., Castelle, B., Parisot, J.-P., Capo, S., Bujan, S., Howa, H., 2009. Morphodynamic response of a meso- to macro-tidal intermediate beach based on a long-term data set. *Geomorphology* 107, 263–274.
- Smith, J.A., Largier, J.L., 1995. Observations of nearshore circulation: rip currents. *Journal of Geophysical Research* 100 (C6), 10967–10975.
- Sonu, C.J., 1972. Field observation on nearshore circulation and meandering currents. *Journal of Geophysical Research* 77, 3232–3247.
- Thornton, E.B., MacMahan, J.H., Sallenger Jr., A.H., 2007. Rips currents, mega-cusps, and eroding dunes. *Marine Geology* 240, 151–167.
- van Maanen, B., de Ruiter, P.J., Coco, G., Bryan, K.R., Ruessink, B.G., 2008. Onshore sandbar migration at Tairua beach (New Zealand): numerical simulations and field measurements. *Marine Geology* 253, 99–106.
- Wright, L.D., Short, A.D., 1984. Morphodynamic variability of surfzone and beaches: a synthesis. *Marine Geology* 56, 93–118.